Vision and Strategies for Reinforcing Additively Manufactured Concrete Structures

Reinforcing Materials

https://doi.org/10.52825/ocp.v1i.75

Submitted: 30 Sept. 2021 | Accepted: 4 Feb. 2022 | Published: 15 Feb. 2022

Combining Wire and Arc Additive Manufacturing and Selective Paste Intrusion for Additively Manufactured Structural Concrete

Fundamental Investigations on the Effect of Heat Exposure by WAAM on the Rheological and Intrusion Behavior of Cement Paste in the Particle Bed During Selective Paste Intrusion

Alexander Straßer[1][https://orcid.org/0000-0003-0293-3392], Daniel Weger[2][https://orcid.org/0000-0003-3762-5592], Carla Matthäus[1][https://orcid.org/0000-0001-9079-8578], Thomas Kränkel[1][https://orcid.org/0000-0002-5650-3825], and Christoph Gehlen[1][https://orcid.org/0000-0002-1214-3960]

[1] Technical University of Munich; Chair of Materials Science and Testing, Germany

[2] Ingenieurbüro Schiessl Gehlen Sodeikat GmbH, Germany

Abstract: The Selective Paste Intrusion (SPI) is an additive manufacturing method in which thin layers of aggregates are bound selectively by cement paste only where the structure shall arise. In this way, concrete elements with complex geometries and structures can be produced. To meet the optimum between required layer bonding and sufficient shape accuracy, the rheological properties of the cement paste, i.e., its yield stress and dynamic viscosity, are crucial [1, 2]. The combination of the SPI process and the Wire and Arc Additive Manufacturing (WAAM) process enables the production of free-formed, high-strength reinforced concrete elements, which opens up a wide range of applications. However, the WAAM process generates high temperatures, which affect the rheological properties of the cement paste and thus the printing quality [3, 4]. Therefore, we analyzed the effect of external temperature loads on the rheological performance of cement paste over the entire SPI production period and derived a maximum acceptable temperature load for the combination of SPI and WAAM. The experiments showed decreasing viscosity and increasing yield stress values by stepwise increasing the paste temperature from 20 °C to 60 °C. Between 60 °C and 70 °C, the rheological behavior suddenly changed, and both viscosity and yield stress instantly increased to a multiple of their initial values. In a subsequent numerical simulation of the intrusion behavior of the paste in the particle bed, we could show that the high yield stress and viscosity lead to poor paste penetration and thus insufficient layer bonding, whereas paste temperatures up to 60 °C are not detrimental to the SPI process. Therefore, the results demonstrate that the combination of SPI and WAAM is possible if the WAAM process is adjusted by e.g. cooling strategies, increased distance of the welding point from the particle bed, or increased time intervals between the welding points to avoid paste temperatures exceeding 60 °C.

Keywords: Additive Manufacturing; Concrete; Particle-Bed; Selective Paste Intrusion; Reinforcement; Wire and Arc Additive Manufacturing; SPI; WAAM; Rheology; Temperature

Conference presentation video: https://doi.org/10.5446/56112

Introduction

Free and complex geometries are often expensive or impossible to realize by conventional manufacturing methods due to the complicated and sometimes even impossible construction of suitable formworks. However, introducing additive, layer-by-layer-based manufacturing techniques make such geometries possible and cheaper to build since there is no need for formwork [5]. The Selective Paste Intrusion (SPI) is such an additive manufacturing method for concrete elements. Compared to other additive manufacturing processes with concrete, such as extrusion or shotcrete, nearly any overhangs are possible [3, 5]. Thereby cement paste is applied to locally bind layers of aggregates. For good penetration behavior, the cement paste needs a constant high flowability over the entire production period. The sufficient penetration behavior is crucial for both a good layer bonding and a satisfying shape accuracy [3, 5–9]. A simple and easy-to-handle test to determine the flowability of the cement paste is the mini-slump flow [10, 11].

In order to improve the mechanical properties and the durability of the concrete components, the SPI process can be supplemented by the integration of steel reinforcement [4]. One possibility is to conventionally insert steel. However, this involves several challenges: prior placement of a reinforcement cage is not possible due to the layer-by-layer production process of SPI, the insertion of reinforcement must be aligned with the open time of the cement paste, and geometrical freedom is restricted. Instead, the reinforcement can also be created additively parallel to the SPI process, which allows the geometric freedom to be retained. Wire and Arc Additive Manufacturing (WAAM), in which molten drops of steel are welded together, can be used to produce steel bars additively with variable diameters and curved structures [12]. As the steel has to be melted for a new layer, high temperature loads are generated at the welding point affecting the surrounding particle bed and thus the intrusion behavior of the cement paste. At the welding point approx. 1500 °C are reached. The temperature decreases over the length of the rebar [4].

First preliminary investigations to determine the temperature load up to which the implementation of WAAM in the SPI process is possible were already carried out by Weger et al. [4]. The tests served as a first rough assessment of the feasibility of combining SPI and WAAM. The investigations showed that increased temperatures could contribute to the cement paste becoming less flowable. This reduces the penetration depth of the cement paste into the particle bed and thus the layer bonding. The yield stress in particular is decisive for the penetration behavior of the cement paste [3]. Therefore, it is necessary to establish improved paste mixtures optimized to almost constant yield stress values over the entire SPI production period and evaluate their yield stress development at increased temperatures. These investigations are essential primarily to enable a combined implementation of SPI and WAAM in practice and secondly for the dimensioning of cooling strategies for this combined additive manufacturing process.

Materials and Methods

Investigations were performed with a reference cement paste, consisting of an ordinary Portland cement with a strength class of 42.5 N, demineralized water, and a composite of three different polycarboxylate ether-based superplasticizers (SP). The mixture was a result of previous investigations to optimize the flowability over longer times. In the preliminary investigation, only the combination of the three SP used resulted in a constant yield stress over 180 min, which corresponds to the production period of the SPI process. The water-to-cement ratio of the paste was 0.3. Mixing was done in a laboratory mixer, operated at 2500 rpm and 4.2 Nm torque. The cement was weighed and added to the mixer. Then the water and the superplasticizer were weighed in together. The water-superplasticizer blend was added to the cement in the mixer, and the mixing process was started for 1:30 min, paused for 2:00 min, and then operated again for 1:30 min at the same speed.

Investigations by Weger [3] show that a mini-slump flow of 400 mm provides sufficiently high penetration depths for the SPI process using aggregates with an average diameter d_{50} between 1.0 mm and 2.6 mm. Therefore, the cement paste was adjusted to 400 mm ± 5 mm mini-slump flow through the dosage of SP. The mini-slump test was only used as a control measure to ensure constant initial flowability of the paste before the rheological characterization. Rheological measurements were done 15:30 min after water addition using a rotational rheometer with parallel plate measuring system.

In addition, the mini-slump flow test can be used to validate the yield stress derived from the rheometer tests [10, 11]. At 14:10 min, the cement paste was remixed with a hand mixer for 30 s so that the mini-slump test could be performed after 15:00 min. The schedule of laboratory activities is shown in Table 1.

In the presentation of results, the yield stress value of the reference cement paste at 20 °C calculated by the Herschel-Bulkley (HB) analysis is therefore compared with the yield stress according to Roussel [10, 11] at 400 mm ± 5 mm mini-slump flow.

Table 1. Schedule of laboratory operations

Time [mm:ss]	Operation
00:00	start mixing
01:30	pause mixing
03:30	start mixing
05:00	stop mixing
14:10	start remixing
14:40	stop remixing
15:00	mini-slump test
15:30	rheological measurement
15:32	stop rheological measurement

The cement paste was rheologically characterized at constant temperatures between 20 °C and 70 °C, in steps of 10 °C each. The temperature after mixing was 20 °C ± 0.5 °C for all pastes, and the temperature was increased to the desired level directly in the rheometer within a few seconds with the aid of a directly heated lower plate of the measuring system and an additional peltier hood (see Figure 1). This peltier hood also ensures a constant temperature during the measurement. Three individual tests were carried out for each temperature load.

Figure 1. Peltier hood installed in the rheometer

Figure 2 shows the used rotational measurement sequence of the rheometer. It consists of a 10 s pre-shear phase at a shear rate of 40 s^{-1} followed by gradually decreasing shear rates between 80 s^{-1} and 0.02 s^{-1}. Every single constant shear rate level lasted for 6 s. During this time, the measured shear stress converged to an almost constant value, representative for the applied shear rate. These shear rates and the corresponding converged shear stresses served for the further calculation of the rheological parameters.

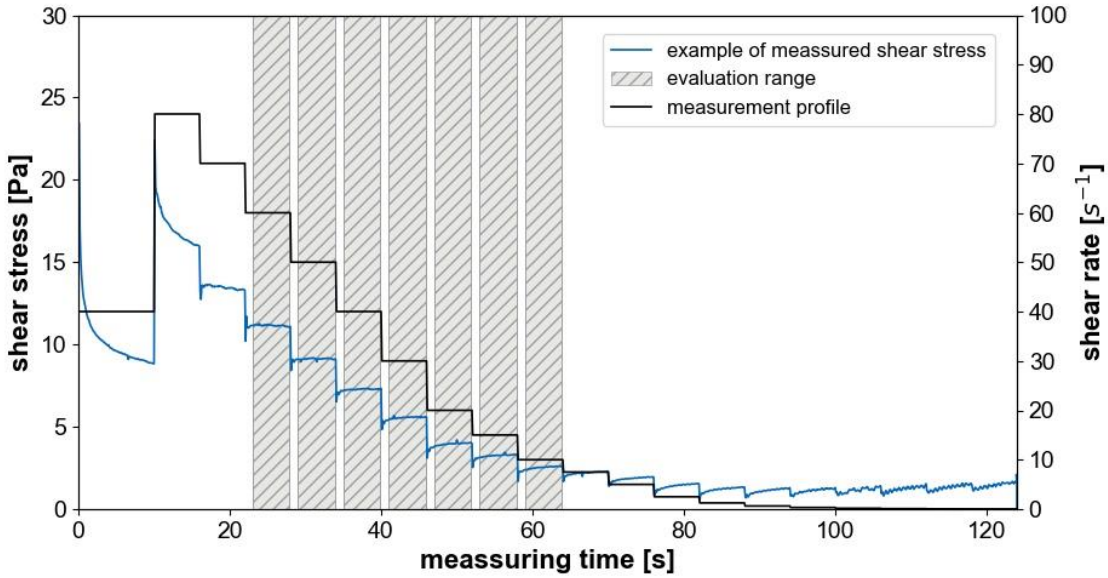

Figure 2. Measurement sequence (black line) and corresponding shear stress of a cement paste (blue line, exemplary) as well as the shear rate range for further evaluation of the rheological parameters (grey shadowed area).

The viscosity was calculated from the quotient of the measured shear stress and the measured shear rate for each measuring point. HB approach was used to calculate the yield stress τ_0, the flow index n, and the consistency index k based on the shear rates between 60 s^{-1} and 10 s^{-1} and the corresponding shear stresses using equation (1) [13, 14].

$$\tau = \tau_0 + k \cdot \dot{\gamma}^n \quad (1)$$

Parameters τ_0, n, and k were calculated in an iterative manner by minimizing the mean squared error between the calculated and the measured shear stresses. Shear rates outside 10 s^{-1} to 60 s^{-1} were excluded from further calculations since the shear stress did not converge to a constant value for the corresponding shear rate, see Figure 2. This indicates structural changes in the paste matrix (further structural breakdown at high shear and structural build-up at low shear). When calculating the mean shear stress values per step, the first and last second were neglected in order to avoid the influence of the shear rate change.

In addition to the direct rheometer measurement, the normal force between the plates was also observed. The normal force was tared at the beginning of the measurement, and the value at the end of the rotational measurement sequence was recorded.

Results and discussion

Shear stress and viscosity

Table 2 shows the measured shear stresses in the evaluated shear rate range between 10 s^{-1} and 60 s^{-1} for the investigated paste temperatures.

Table 2. Measured shear stresses for corresponding shear rates of the cement paste at paste temperatures between 20 °C and 70 °C.

Paste temperature [°C]	Shear rate [s^{-1}]						
	10	15	20	30	40	50	60
	Shear stress [Pa]						
20	2.3	3.1	4.0	5.8	8.0	10.3	13.0
30	2.1	2.7	3.3	4.8	6.5	8.4	10.5
40	2.1	2.7	3.2	4.6	6.3	8.2	10.4
50	2.1	2.5	2.9	4.0	5.3	6.9	8.7
60	2.1	2.4	2.7	3.7	4.7	6.1	7.6
70	14.9	13.4	12.4	12.8	13.3	13.6	14.2

Between 20°C and 60°C, the shear stresses of the cement paste tend to decrease with increasing temperature at the respective shear rate. Moreover, the shear stresses of the samples in that temperature range differ significantly less in the low shear rate range than in the high shear rate range. With increasing shear rate, the shear stresses, therefore, develop under proportionally with increasing paste temperature up to 60 °C, which indicates a decreasing viscosity of the cement paste with increasing temperature. This can also be seen in Figure 3, where the dynamic viscosities are shown as the ratio of applied shear rate to measured shear stress for the paste temperatures investigated.

In investigations by Lee et al. [15], this decrease in viscosity with increasing temperature attributes to increasing Brownian motion. Lee et al. [15] carried out rheological investigations with cement pastes between 5 °C and 40 °C and showed this behavior in agreement with the results presented here. The higher the temperature, the lower the viscosity. The higher the temperature, the faster the molecules can move in the cement paste suspension.

The binding forces between the molecules decreases, and in turn, the distance between the cement particles increases. Thus, the flow resistance decreases in this temperature range. [15–17]

Furthermore, the cement pastes showed slightly shear-thinning behavior in the low-shear range up to 30 s^{-1} – 40 s^{-1} and switched afterward to slightly shear thickening behavior for increased shear. This is valid for every investigated temperature up to 60 °C. The ob-

served behavior can be related to the fact that the particles in the cement paste start moving at low shear rates, and their distance to each other in shear direction increases due to steric and electrostatic repulsion as well as particle alignment. This causes shear-thinning behavior. Increasing the shear stress causes pronounced particle collisions in the cement paste so that the shear-thinning behavior gradually turns into shear-thickening behavior. [18]

Summarizing the viscosity values up to a paste temperature of 60 °C, it can be concluded that the viscosity in this range does not increase, but even decreases slightly. This corresponds to a slight improvement with regard to the requirements in the SPI process, especially for conveying the cement paste through the nozzles. Furthermore, this is an important aspect regarding the SPI process requirements of a stable and constant viscosity during the printing period.

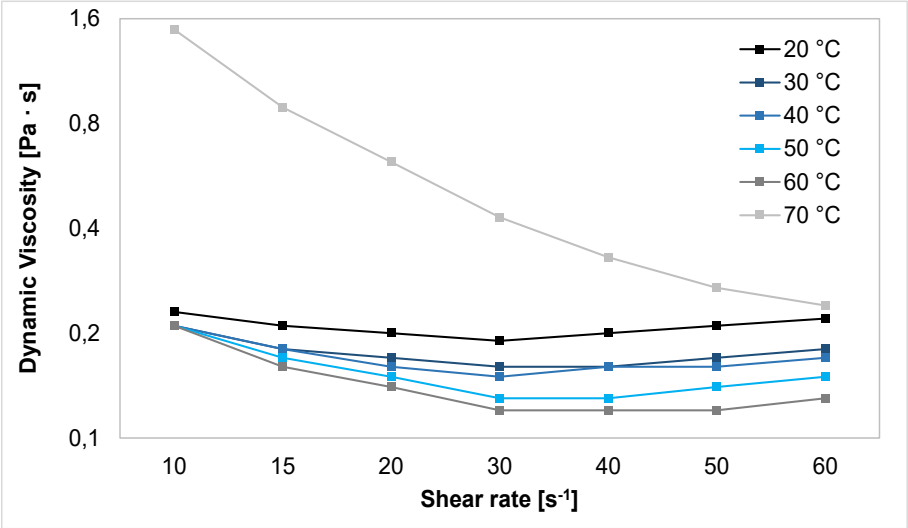

Figure 3. Viscosity curve of the cement paste at a paste temperature range from 20 °C to 70 °C.

At 70 °C, the results of the rheological measurements of the cement paste deviate from all observations made at lower temperatures. At 70 °C, the cement paste exhibits generally higher shear stresses (see Table 2) and thus shows increased dynamic viscosities (Figure 3) compared to the other mixtures at 60 °C or lower.

We assume that at a temperature increase from 60 °C to 70 °C, phase instabilities occur that lead to a change in the rheological behavior of the cement paste. At a temperature of somewhat below 70 °C, the decomposition (dehydration) of the early-built ettringite ($Ca_6Al_2(SO_4)_3(OH)_{12}\cdot 26\ H_2O$), which formed directly after the addition of water to the cement, might occur. Ettringite is known to become unstable at temperatures above approx. 50 °C [19–23], while the exact phase stability depends among others on the Al_2O_3/SO_3 ratio in the system [20, 24, 25]. Once ettringite is unstable, the sulfate and aluminum ions are probably forced to form layered double hydroxides instead of ettringite, or more specifically AFm phases, such as monosulphate. Such plate-shaped hydrates might build up a card-house structure, which could explain the sudden setting of the cement paste and thus the subsequent increase in viscosity. In addition, at 70 °C, the paste showed strong shear-thinning behavior over the entire range of shear rate evaluated. This indicates that an increased shear force is able to destroy the card-house-structure of AFm phases.

More detailed investigations to elucidate this behavior are currently being carried out. In further research, the interactions of the SP will also be investigated and a non-reactive, blank sample will be tested.

Normal force

In addition to the rheological parameters, the normal force between the plates was recorded during the rheometer measurement sequence. In the case of possible evaporation of water from the cement paste at increasing temperatures, the paste volume would decrease and with it the gap between the plates. Since the gap width between the plates was kept constant during the entire measurement sequence, water evaporation is indicated by a decreasing normal force. The measured normal forces after finishing the rheometer measurement can be taken from Table 3. By taring the values at the beginning of the measurement, tensile forces are displayed as negative values.

Table 3. Normal forces after rheometer measurement as a function of paste temperature

Temperature [°C]	Normal Force [N]
20	-0.08
30	-0.09
40	-0.07
50	-0.11
60	-0.17
70	-7.34

While the normal force is almost zero for all measurements conducted at temperatures up to 60°C, there is a sudden increase in tensile force from 60°C to 70°C. The pronounced tensile value at 70°C also indicates a change in the phase assemblage, as ettringite is a rather voluminous hydrate compared to AFm phases. However, the decomposition of ettringite or the transformation of ettringite to AFm phases would also cause the release of a significant amount of water. Therefore, more in-depth analyses on the amount of ettringite formed at lower temperatures and the amount of AFm phases formed at 70 °C need to be carried out in order to account for the volume of the various states of water (free water or bound water) and the volume of solid phases in the systems at various temperatures.

Calculation of yield stress, flow index, and consistency index

The calculated yield stresses, flow indices, consistency index, and related mean squared errors are presented in **Table 4**.

Table 4. Calculated Herschel-Bulkley parameter. Yield stress, flow index, consistency index, and mean squared error (MSE) for varying paste temperature.

Temperature [°C]	Yield stress $\dot{\gamma}$ [Pa]	Flow index n [-]	Consistency index k [-]	MSE [-]
20	1.4	1.38	0.040	0.006
30	1.5	1.46	0.023	0.006
40	1.6	1.52	0.017	0.004
50	1.7	1.62	0.009	0.003
60	1.8	1.66	0.006	0.002
70	13.3	4.42	0.000	3.703

To verify whether the calculated yield stresses are appropriate, the yield stress according to Roussel [10, 11] at a mini-slump flow of 400 mm ± 5 mm is compared to the yield stress according to the HB analysis at 20 °C. A mini-slump flow of 400 mm ± 5 mm corresponds according to Roussel [10, 11] to a yield stress range of 1.28 Pa to 1.45 Pa. The reference cement paste at 20 °C with 1.4 Pa is therefore in this range.

The yield stress and the flow index slightly increase with increasing temperature up to 60 °C. One possible explanation would be the evaporation of water. However, the effect on the yield stress is relatively high in relation to the small temperature increase from 60 °C to 70 °C. Therefore, this behavior could also be due to an already accelerated hydration caused

by the temperature. [26–28] However, a significant increase can be seen only at a temperature of 70 °C, which might be linked to the phase instabilities already described.

Effect of rheological parameters in the practical application of SPI

Weger and Gehlen [1] showed that an optimum between the layer thickness of the aggregates and the penetration depth of the cement paste must be found in order to achieve both sufficient material properties (strength, durability) and shape accuracy in the production of SPI structures.

The penetration depth of the cement paste into the particle bed depends on the rheological properties of the cement paste and the flow resistance of the particle bed. To avoid the effort of "trial and error" tests, Pierre et al. [7, 29] and Weger et al. [2] developed calculation and simulation models to predict the penetration depth of cement pastes in the SPI process.

Under the assumption of a particle bed with an average aggregate diameter d_{50} of 1.0 mm, 1.6 mm as well as 2.6 mm and the measured rheological parameters of the investigated cement pastes, see Table 4 the penetration depth of the cement paste can be calculated using Eq. 1 [2].

$$e = \frac{\rho_P \cdot g \cdot \frac{H_{0,eff}}{2} \cdot d_{eff} \cdot \varepsilon}{\tau_0 + \frac{\tau_{0,lim}}{\tau_0} \cdot k \cdot \dot{\gamma}^n} \tag{2}$$

Where e (m) is the penetration depth of the cement paste into the particle bed, ρ_p (kg m-3) is the density of the cement paste, g (m s^{-2}) is the gravitational constant, $H_{0,eff}$ (m) is the effective height of the cement paste determining the maximum initial hydrostatic pressure acting at the bottom of the cement paste, d_{eff} (m) is the effective diameter of the capillary pore system of the particle bed, ε is the porosity of the particle-bed, τ_0 is the Herschel-Bulkley yield stress (Pa), $\tau_{0,lim}$ is the limiting yield stress (Pa), k is the Herschel-Bulkley consistency index (-), $\dot{\gamma}$ (s^{-1}) is the shear rate of the penetrating cement paste in a pressure less capillary pore system and n (-) is the Herschel-Bulkley flow index. Figure 4 shows the predicted penetration depths following Eq. (2).

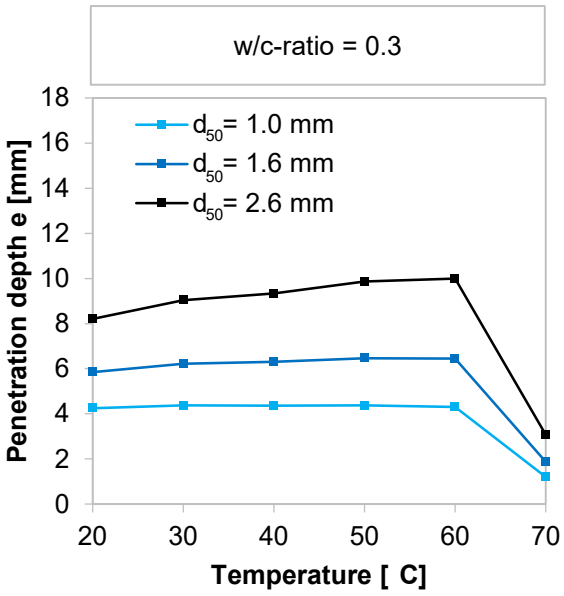

Figure 4. Penetration depth e of the cement paste in dependency of the temperature of the cement paste following Eq. 2 [2]

On the one hand, the results show an increasing penetration depth of the cement paste with increasing average diameter d_{50} of the particles in the particle bed due to a decreasing flow resistance [1–3, 5–9]. On the other hand, the results exhibit an increasing penetration depth up to a cement paste temperature of 60 °C, although the yield stress is almost constant, and the flow index n is slightly increasing. This can be explained by the simultaneously decreasing viscosity and consistency index k. Furthermore, the increase in penetration depth with temperature is more pronounced with increasing d_{50}, while the particle bed with a d_{50} of 1.0 mm exhibits a quite constant penetration depth up to 60 °C. This is probably caused by the increasing flow resistance of the particle bed and therefore limited free flow of the cement paste into the voids between the particles. This effect limits the influence of the viscosity and increases the impact of the yield stress on penetration depth [2, 3].

However, at 70 °C, the penetration depths strongly decrease at all investigated aggregate sizes. This can be explained by the strong increase of the yield stress and the apparent viscosity due to the first decomposition (dehydration) of the early-built ettringite and the related built-up of plate-shaped hydrates, which itself might build up a card-house structure (see results of apparent viscosity measurements above).

Related to a practical application, the prediction acc. Eq. (1) shows that the temperature should have an effect on the penetration depth and, therefore, on the maximum possible layer thickness in the SPI printing process. Assuming a layer thickness of 3 ± 2 mm, a sufficient layer bonding should be achieved up to a temperature of 60 °C. However, using a d_{50} of 2.6 mm shape accuracy could decrease with increasing temperature. As soon as a temperature of 70 °C is reached, the penetration depth decreases to 1.2 mm (d_{50} = 1.0 mm), 1.9 mm (d_{50}=1.6 mm) and 3.1 mm (d_{50} = 2.6 mm). Therefore, when WAAM is used at the same time, it will be essential to limit the cement paste temperature by additional cooling strategies for the printing process.

It should be noted that a printer with a nozzle diameter of 2 mm was assumed. The technology of the SPI printer is further under development, and the nozzle diameter might change in the future. It must be taken into account that the penetration behavior is, besides the cement paste rheology, also linked to the printer setting (i.e., the nozzle diameter) and the characteristics of the particle bed (i.e., particle diameter, shape, and packing density/porosity). Therefore, the calculations may have to be repeated if these parameters are changed.

Conclusions

The additive manufacturing method Selective Paste Intrusion (SPI) is combined with Wire and Arc Additive Manufacturing (WAAM) to produce a steel reinforcement in SPI elements. The WAAM process will generate heat in the reinforcing steel, transferred to the surrounding cement paste in the particle bed [4].

In the SPI process, the rheological properties of the cement paste are of high significance. They affect the printing quality of the components. Thus, yield stresses smaller than limiting yield stress, which depends on the flow resistance of the particle bed, must be aimed [3, 7]. Since external temperature loads influence the rheological properties of cement pastes, the critical temperature threshold was determined at temperatures above 60 °C. Up to this temperature, the yield stresses were between 1.41 and 1.80 Pa and should thus allow sufficient penetration depths. It can be assumed that temperature loads up to at least 60 °C are permissible. The fact that viscosity decreases with increasing temperature load is a positive side effect. However, the temperature load must not be higher than 70 °C. The range between 60 °C and 70 °C can still be investigated in further tests. The findings obtained will help to develop cooling strategies and the design of a cooling system to keep the temperature loads in the particle bed to a minimum. Furthermore, based on them, the combined SPI-WAAM process can be designed, including the distance between the welding point and the

powder bed as well as the maximum feasible speeds of the layer production, thus achieving a further step towards reinforced, high-strength concrete elements.

Outlook

Future investigations are planned to take a closer look at the critical range between 60 °C and 70 °C by starting a new series with, for example, an increment of 2 °C.

It is also conceivable to optimize the cement paste formulation. Initial discussions with producers of chemicals for the building materials industry revealed that additional additives, such as retarders or super absorbing polymers, could make the cement paste more resistant to external temperature loads.

In addition, printing tests will be carried out on the SPI printer. Here, both the performance of the cement paste and the process stability towards increased temperature loads are to be investigated and optimized.

Data availability statement

The data are not published. In case of interest, the corresponding author (alexander.strasser@tum.de) will provide the data upon request.

Author contributions

Conceptualization, A.S.; methodology, A.S.; validation, A.S.; formal analysis, A.S.; investigation, A.S.; writing—original draft preparation, A.S., D.W.; writing—review and editing, A.S., D.W., C.M., T.K.; visualization – Figures 1, 2 and 3, A.S., Figure 4, D.W.; supervision, C.M., T.K.; project administration, C.M., T.K.; funding acquisition, C.G. All authors have read and agreed to the published version of the manuscript

Competing interests

The authors declare no competing interests.

Funding

This research was funded by the Deutsche Forschungsgemeinschaft (DFG, German Research Foundation) – Project-number 414265976 – TRR 277

Acknowledgment

The authors would like to thank Prof. Alisa Machner and Dr. Anne Heisig, Chair of Mineral Construction Materials, Technical University of Munich, for their support and fruitful discussion regarding the chemical changes of cement paste at elevated temperatures.

References

1. Weger, D. and Gehlen, C. 2021. Particle-Bed Binding by Selective Paste Intrusion-Strength and Durability of Printed Fine-Grain Concrete Members. Materials (Basel, Switzerland) 14, 3. DOI: https://doi.org/10.3390/ma14030586.

2. Weger, D., Pierre, A., Perrot, A., Kränkel, T., Lowke, D., and Gehlen, C. 2021. Penetra-tion of Cement Pastes into Particle-Beds: A Comparison of Penetration Models. Mate-rials (Basel, Switzerland) 14, 2. DOI: https://doi.org/10.3390/ma14020389.
3. Weger, D. 2020. Additive Fertigung von Betonstrukturen mit der Selective Paste Intru-sion – SPI / Additive manufacturing of concrete structures by Selective Paste Intrusion - SPI. Dissertation, Munich.
4. Weger, D., Baier, D., Straßer, A., Prottung, S., Kränkel, T., Bachmann, A., Gehlen, C., and Zäh, M. Reinforced Particle-Bed Printing by Combination of the Selective Paste In-trusion Method with Wire and Arc Additive Manufacturing – A First Feasibility Study 28, 978–987. DOI: https://doi.org/10.1007/978-3-030-49916-7_95.
5. Weger, D., Gehlen, C., Lowke, D. Additive Fertigung von Betonbauteilen durch selekti-ve Zementleim-Intrusion. Proceedings of Ibausil 2018.
6. Lowke, D., Dini, E., Perrot, A., Weger, D., Gehlen, C., and Dillenburger, B. 2018. Parti-cle-bed 3D printing in concrete construction – Possibilities and challenges. Cement and Concrete Research 112, 50–65. DOI: https://doi.org/10.1016/j.cemconres.2018.05.018.
7. Pierre, A., Weger, D., Perrot, A., and Lowke, D. 2018. Penetration of cement pastes into sand packings during 3D printing: analytical and experimental study. Mater Struct 51, 1. DOI: https://doi.org/10.1617/s11527-018-1148-5.
8. Weger, D., Lowke, D., Gehlen, C. 3D Printing of Concrete Structures with Calcium Sili-cate based Cements using the Selective Binding Method - Effects of Concrete Tech-nology on Penetration Depth of Cement Paste. Proceedings of Hipermat 2016 - 4th In-ternational Symposium on Ultra-High Performance Concrete and High Performance Construction Materials 2016.
9. Weger, D., Lowke, D., Gehlen, C., Talke, D., Henke, K. Additive manufacturing of con-crete elements using selective cement paste intrusion – effect of layer orientation on strength and durability. Proceedings of RILEM 1st International Conference on Con-crete and Digital Fabricaton 2018.
10. Roussel, N. and Coussot, P. 2005. “Fifty-cent rheometer” for yield stress measurements: From slump to spreading flow. Journal of Rheology 49, 3, 705–718. DOI: https://doi.org/10.1122/1.1879041.
11. Roussel, N., Stefani, C., and Leroy, R. 2005. From mini-cone test to Abrams cone test: measurement of cement-based materials yield stress using slump tests. Cement and Concrete Research 35, 5, 817–822. DOI: https://doi.org/10.1016/j.cemconres.2004.07.032.
12. Mechtcherine, V., Grafe, J., Nerella, V. N., Spaniol, E., Hertel, M., and Füssel, U. 2018. 3D-printed steel reinforcement for digital concrete construction – Manufacture, me-chanical properties and bond behaviour. Construction and Building Materials 179, 125–137. DOI: https://doi.org/10.1016/j.conbuildmat.2018.05.202.
13. Larrard, F. de, Ferraris, C. F., and Sedran, T. 1998. Fresh concrete: A Herschel-Bulkley material. Mater Struct 31, 7, 494–498. DOI: https://doi.org/10.1007/BF02480474.
14. Mezger, T.G. 2006. Das Rheologie Handbuch. Für Anwender von Rotations- und Oszil-lations-Rheometern. Vincentz, Hannover, Germany.
15. Lee, D. K. and Choi, M. S. 2018. Standard Reference Materials for Cement Paste: Part III-Analysis of the Flow Characteristics for the Developed Standard Reference Material According to Temperature Change. Materials (Basel, Switzerland) 11, 10. DOI: https://doi.org/10.3390/ma11102001.
16. Martini, S. A. and Nehdi, M. 2009. Coupled Effects of Time and High Temperature on Rheological Properties of Cement Pastes Incorporating Various Superplasticizers. J. Mater. Civ. Eng. 21, 8, 392–401. DOI: https://doi.org/10.1061/(ASCE)0899-1561(2009)21:8(392).
17. Wang, Y., Wu, A., Ruan, Z., Wang, H., Wang, Y., and Jin, F. 2018. Temperature Effects on Rheological Properties of Fresh Thickened Copper Tailings that Contain Cement. Journal of Chemistry 2018, 1–8. DOI: https://doi.org/10.1155/2018/5082636.

18. Haist, M. 2010. Zur Rheologie und den physikalischen Wechselwirkungen bei Zementsuspensionen. Dissertation. Zugl.: Karlsruhe, Univ., Diss., 2009. Karlsruher Reihe Massivbau, Baustofftechnologie, Materialprüfung H. 66. KIT Scientific Publ, Karlsruhe.
19. Gallucci, E., Zhang, X., and Scrivener, K. L. 2013. Effect of temperature on the microstructure of calcium silicate hydrate (C-S-H). Cement and Concrete Research 53, 185–195. DOI: https://doi.org/10.1016/j.cemconres.2013.06.008.
20. Lothenbach, B., Winnefeld, F., Alder, C., Wieland, E., and Lunk, P. 2007. Effect of temperature on the pore solution, microstructure and hydration products of Portland cement pastes. Cement and Concrete Research 37, 4, 483–491. DOI: https://doi.org/10.1016/j.cemconres.2006.11.016.
21. Kjellsen, K. O. and Detwiler, R. J. 1992. Reaction kinetics of portland cement mortars hydrated at different temperatures. Cement and Concrete Research 22, 1, 112–120. DOI: https://doi.org/10.1016/0008-8846(92)90141-H.
22. Damidot, D. and Glasser, F. P. 1992. Thermodynamic investigation of the CaO-Al2O3-CaSO4-H2O system at 50°C and 85°C. Cement and Concrete Research 22, 6, 1179–1191. DOI: https://doi.org/10.1016/0008-8846(92)90047-y.
23. Perkins, R. B. and Palmer, C. D. 1999. Solubility of ettringite (Ca6[Al(OH)6]2(SO4)3 · 26H2O) at 5–75°C. Geochimica et Cosmochimica Acta 63, 13-14, 1969–1980. DOI: https://doi.org/10.1016/S0016-7037(99)00078-2.
24. Lothenbach, B., Matschei, T., Möschner, G., and Glasser, F. P. 2008. Thermodynamic modelling of the effect of temperature on the hydration and porosity of Portland cement. Cement and Concrete Research 38, 1, 1–18. DOI: https://doi.org/10.1016/j.cemconres.2007.08.017.
25. Deschner, F., Lothenbach, B., Winnefeld, F., and Neubauer, J. 2013. Effect of temperature on the hydration of Portland cement blended with siliceous fly ash. Cement and Concrete Research 52, 169–181. DOI: https://doi.org/10.1016/j.cemconres.2013.07.006.
26. Nehdi, M. and Al Martini, S. 2009. Estimating time and temperature dependent yield stress of cement paste using oscillatory rheology and genetic algorithms. Cement and Concrete Research 39, 11, 1007–1016. DOI: https://doi.org/10.1016/j.cemconres.2009.07.011.
27. Nehdi, M. and Al Martini, S. 2007. Effect of Temperature on Oscillatory Shear Behavior of Portland Cement Paste Incorporating Chemical Admixtures. J. Mater. Civ. Eng. 19, 12, 1090–1100. DOI: https://doi.org/10.1061/(ASCE)0899-1561(2007)19:12(1090).
28. Varshney, A., Gohil, S., Chalke, B. A., Bapat, R. D., Mazumder, S., Bhattacharya, S., and Ghosh, S. 2017. Rheology of hydrating cement paste: Crossover between two ag-ing processes. Cement and Concrete Research 95, 226–231. DOI: https://doi.org/10.1016/j.cemconres.2017.02.034.
29. Pierre, A., Weger, D., Perrot, A., and Lowke, D. 2020. Additive Manufacturing of Cementitious Materials by Selective Paste Intrusion: Numerical Modeling of the Flow Using a 2D Axisymmetric Phase Field Method. Materials (Basel, Switzerland) 13, 21. DOI: https://doi.org/10.3390/ma13215024.